Density functional study for crystalline structures and electronic properties of $Si_{1-x}Sn_x$ binary alloys

Yuki Nagae[*1], Masashi Kurosawa[1, 2, 3], Shigehisa Shibayama[1, 4, †], Masaaki Araidai[1, 2, 3], Mitsuo Sakashita[1], Osamu Nakatsuka[1], Kenji Shiraishi[1, 3], and Shigeaki Zaima[1, 3]

[1]*Graduate School of Engineering, Nagoya University, Nagoya 464-8603, Japan*
[2]*Institute for Advanced Research, Nagoya 464-8603, Japan*
[3]*Institute of Materials and Systems for Sustainability, Nagoya 464-8603, Japan*
[4]*Research Fellow of the Japan Society for the Promotion of Science, Chiyoda, Tokyo, 102-0083, Japan*

[†]Present address: The University of Tokyo, Bunkyo Tokyo 113-8656, Japan

*E-mail: ynagae@alice.xtal.nagoya-u.ac.jp

Abstract

We have carried out density functional theory (DFT) calculation for $Si_{1-x}Sn_x$ alloy and investigated the effect of the displacement of Si and Sn atoms with strain relaxation on the lattice constant and E-$\boldsymbol{k}$ dispersion. We calculated the formation probabilities for all atomic configurations of $Si_{1-x}Sn_x$ according to the Boltzmann distribution. The average lattice constant and E-$\boldsymbol{k}$ dispersion were weighted by the formation probability of each configuration of $Si_{1-x}Sn_x$. We estimated the displacement of Si and Sn atoms from the initial tetrahedral site in the $Si_{1-x}Sn_x$ unit cell considering structural relaxation under hydrostatic pressure, and we found that the breaking of the degenerated electronic levels of the valence band edge could be caused by the breaking of the tetrahedral symmetry. We also calculated the E-$\boldsymbol{k}$ dispersion of the $Si_{1-x}Sn_x$ alloy by the DFT+U method and found that a Sn content above 50% would be required for the indirect-direct transition.

1 **1. Introduction**

2 Group-IV semiconductor alloys are candidate materials of optoelectronic devices for
3 intra- and interchip optical wirings in silicon-based high-performance large-scale
4 integrated circuits.[1–3] Among group-IV alloy semiconductors, the Si-Sn binary alloy
5 ($Si_{1-x}Sn_x$) is an interesting material, since its energy bandgap (E_g) is theoretically
6 expected to correspond to a preferable energy bandgap (E_g=0.75–0.95 eV) for optical
7 communication applications.[4]

8

9 There is a great challenge for the practical application of $Si_{1-x}Sn_x$ because the
10 formation of the $Si_{1-x}Sn_x$ alloy with an appreciably high Sn content is quite difficult
11 owing to the low thermal equilibrium solubility of Sn in Si (~0.1%). There are a few
12 reports on the crystal growth of $Si_{1-x}Sn_x$.[5–7] Recently, we have experimentally achieved
13 the formation of poly $Si_{1-x}Sn_x$ layers on an insulator with a Sn content as high as 18±4%
14 and succeeded in determining that the direct and indirect E_g values are 0.83 and 1.05 eV,
15 respectively, from the result of Fourier transform infrared spectroscopy.[8] However, the
16 details of the crystalline and electronic properties of the $Si_{1-x}Sn_x$ alloy, such as the Sn
17 content dependence of the energy bandgap of $Si_{1-x}Sn_x$, the Sn content of the
18 indirect-direct crossover, and the effect of stress due to the introduction of Sn into Si on
19 the electronic states, have not been understood yet.

20

21 On the other hand, there are some reports on theoretical calculations related to the
22 energy band structure of $Si_{1-x}Sn_x$.[6, 9–11] Theoretical calculation predicted the
23 indirect-direct crossover at a Sn content (x_{dir}) of $Si_{1-x}Sn_x$.[6] Tolle *et al.* used local density
24 approximation with Sn-content-dependent *scissors correction* for the 64-atom unit cell

1 of $Si_{1-x}Sn_x$ and then found x_{dir}=32%.[9] Moontragoon *et al.* determined that x_{dir}=55% by
2 using a virtual crystalline approximation of the empirical pseudopotential method for an
3 8-atom unit cell of $Si_{1-x}Sn_x$.[10] These two methodologies are *empirical correction*
4 methods for E_g evaluation. On the other hand, Amrane *et al. unempirically* calculated
5 the x_{dir} of $Si_{1-x}Sn_x$ by using the modified Becke-Johnson exchange-correlation
6 pseudopotential and found that x_{dir}=49% for an 8-atom unit cell.[11] However, there is still
7 an issue about x_{dir}, which is highly variable from 32 to 55%.
8
9 We focus on the effect of the displacement of Si and Sn atoms in the unit cell of the
10 $Si_{1-x}Sn_x$ alloy with strain relaxation on the electronic properties in order to calculate
11 them more correctly. In the case of perovskite crystalline structures, it is well known
12 that the physical characteristics (*i.e.,* super conductivity, magnetic property, electronic
13 transport property, optical property, and dielectric property) are strongly affected by the
14 local displacement of atoms depending on the strain relaxation.[13–16] However, there is
15 no report on the effect of the displacement of atoms on the physical and electronic
16 characteristics of group-IV alloys. Taking into account that a pair of Si and Sn have a
17 larger difference in atomic radius (~20%),[17] the displacement of Si and Sn atoms in the
18 cell should be significant, which should strongly affect the physical characteristics such
19 as the energy band structures of $Si_{1-x}Sn_x$.
20
21 In this study, we calculated the lattice constant of $Si_{1-x}Sn_x$ considering the strain
22 relaxation, which causes the displacement of atoms in $Si_{1-x}Sn_x$. We discussed the effect
23 of the displacement of Si and Sn atoms on the physical and electronic properties of Si_{1-}
24 $_xSn_x$. Also, in our calculation, we considered all configurations of atoms in $Si_{1-x}Sn_x$ to

1 estimate the average lattice constant and energy bandgap of $Si_{1-x}Sn_x$ according to the
2 Boltzmann distribution. We clarified the Sn content dependence of the energy bandgap
3 of $Si_{1-x}Sn_x$.
4

5 **2. Calculation method**

6 The DFT calculation was performed using the PHASE/0 code[18] in order to calculate the
7 lattice constant, formation probability, and E-$\boldsymbol{k}$ dispersions of $Si_{1-x}Sn_x$. We used the
8 generalized gradient approximation (GGA) of the Perdew-Burke-Ernzherhof (PBE)
9 functional for the exchange-correlation potential[19] and projector augmented wave
10 (PAW) potential for the electron-ion interaction.[20] The unit cell was composed of 8
11 atoms in a diamond lattice ($Si_{8-n}Sn_n$, n=0–8, where n is the integer number of Sn atoms
12 in a unit cell). If there are two Sn atoms (n=2) in $Si_{8-n}Sn_n$, the Sn content of $Si_{8-n}Sn_n$
13 corresponds to 25%. For all calculations, a 2×2×2 Monkhorst-Pack grid of $\boldsymbol{k}$-points[21]
14 was applied as well as a plane wave energy cutoff of 500 eV.
15

16 Furthermore, we considered all unique atomic configurations in each $Si_{8-n}Sn_n$ alloy
17 and the formation probability of each configuration according to the Boltzmann
18 distribution. Figures 1(a) and 1(b) show examples of two unique atomic configurations
19 of the Si_6Sn_2 alloy corresponding to a Sn content of 25%, namely, the first nearest
20 neighbor (1NN) and the second nearest neighbor (2NN) of two Sn atoms, respectively.
21 We calculated the lattice constant and its formation energy for all unique $Si_{8-n}Sn_n$
22 configurations by using the GGA-PBE exchange-correlation potential taking into
23 account the structural relaxation of an isotropic stress for a unit cell under hydrostatic
24 pressure.

1

2 The formation energy $E_{\mathrm{form},i}$ of the i-th unique atomic configuration of $Si_{8-n}Sn_n$ for

3 a certain Sn content was calculated as[22]

$$E_{\mathrm{form},i}(n) = E_{\mathrm{total},i}(n) - [E_{\mathrm{total}}(0) - n\mu_{\mathrm{Si}} + n\mu_{\mathrm{Sn}}], \quad (1)$$

4 where $E_{\mathrm{total},i}(n)$ is the total electron energy of an i-th certain unique atomic configuration

5 of $Si_{8-n}Sn_n$ [i.e., $E_{\mathrm{total}}(0)$ is the total electron energy of Si bulk], and μ_{Si} and μ_{Sn} are the

6 chemical potentials of pure Si and α-Sn, which are derived from $E_{\mathrm{total}}(0)/8$ and $E_{\mathrm{total}}(8)/8$,

7 respectively. In this study, we took into account the formation probability according to

8 the Boltzmann distribution in order to evaluate the weighted averages of calculation

9 results such as the lattice constant and energy bandgap.

10

11 For example, the formation energies of two probable configurations including 1NN

12 and 2NN Sn atoms in a Si_6Sn_2 case from Eq. (1) were estimated to be 1.140 and 1.063

13 eV, respectively. The formation energy of the 2NN case is 0.077 eV lower than that of

14 the 1NN case. This result means that the configuration of 1NN is more energetically

15 unstable than that of 2NN, which can be attributed to a larger inner stress due to the

16 nearest-neighbor large Sn atoms in the Si matrix. In this study, we considered the

17 formation probability for each configuration. The formation probability $P_{\mathrm{form},i}(n)$ of an

18 i-th unique atomic configuration of a certain Sn content is evaluated as

$$P_{\mathrm{form},i}(n) = \frac{\exp\left[-\frac{E_{\mathrm{form},i}(n)}{\mathrm{k_B}T}\right]}{\sum_j \exp\left[-\frac{E_{\mathrm{form},j}(n)}{\mathrm{k_B}T}\right]}, \quad (2)$$

19 where $\mathrm{k_B}$ is the Boltzmann constant and T is the absolute temperature. The formation

20 probabilities of 1NN and 2NN cases for the Si_6Sn_2 unit cell were estimated to be 8%

1 and 92%, respectively. We used the formation probability of all configurations for
2 estimating the weighted averages. The crystalline and electrical properties (i.e., total
3 electron energy, lattice constant, and E_g) of each $Si_{8-n}Sn_n$ alloy with various Sn contents
4 were calculated considering all unique atomic configurations.
5

6 ## 3. Results and discussion

7 Figure 2 shows the lattice constant of $Si_{8-n}Sn_n$ as a function of the Sn content. The
8 calculated values for all configurations are shown with open diamonds and the weighted
9 averages are also shown with solid triangles. In addition, the lattice constant according
10 to Vegard's law is shown by a broken line. The lattice constants of Si and α-Sn were
11 estimated to be 5.46 and 6.65 Å, respectively. These values are in reasonable agreement
12 with 5.47 Å for Si[23] and 6.65–6.74 Å for α-Sn[24, 25] previously obtained by the
13 calculation with the GGA-PBE. The calculated lattice constants of $Si_{8-n}Sn_n$ in this study
14 slightly deviated from Vegard's law, meaning that the bowing parameter of the $Si_{1-x}Sn_x$
15 alloy can be negligible compared with those of the $Si_{1-x}Ge_x$ and $Ge_{1-x}Sn_x$ binary alloys.
16 This tendency of $Si_{8-n}Sn_n$ well agrees with previous reports[6, 12]. Tolle *et al.* reported that
17 the bowing parameter of the $Si_{1-x}Sn_x$ alloy can be negligible (0.02%) as determined by
18 the calculation for 64 atoms of a $Si_{0.50}Sn_{0.50}$ random alloy.[6]
19 In addition, it is easily predicted that Si and Sn atoms are displaced from the initial
20 position in a diamond lattice structure by strain relaxation due to the difference in
21 atomic radius between Si and Sn. Therefore, we investigated the displacement of Si and
22 Sn atoms from the tetrahedral sites in the diamond lattice by considering the structural
23 relaxation. In this study, we defined $\mathbf{r}_{k0}$ and $\mathbf{r}_{k,\mathrm{relaxed}}$ as positional vectors for the initial
24 sample and that after structural relaxation, respectively, where k is the index of the k-th

1 atom in a unit cell. The displacement vector $\Delta \boldsymbol{r}_k$ is defined as

$$\Delta \mathbf{r}_k = \mathbf{r}_{k,\mathrm{relaxed}} - \mathbf{r}_{k0}. \quad (3)$$

2 The average displacement $\overline{\Delta r}$ of all atoms in a certain configuration of a $Si_{8-n}Sn_n$ cell
3 was calculated as

$$\overline{\Delta r} = \frac{1}{8}\sum_{k=1}^{8} |\Delta \mathbf{r}_k|. \quad (4)$$

4 $\overline{\Delta r}$ values as a function of the Sn content are shown with open circles in Fig. 3. The
5 weighted averages of displacement calculated by using Eq. (2) are also shown with
6 solid circles in Fig. 3. Those values are on the order of 0.09 Å regardless of the Sn
7 content except for pure Si (n=0) and α-Sn (n=8). This result is strong evidence that the
8 Si and Sn in a $Si_{8-n}Sn_n$ unit cell are displaced from their initial positions in a diamond
9 lattice considering the structural relaxation. This result also suggests that the local
10 internal stress with the difference in atomic radius between Si and Sn in the $Si_{8-n}Sn_n$
11 alloy can be possibly released by the quite low atomic displacement from the initial
12 position.

13 As we mentioned in the introduction, the atomic displacement strongly affects the
14 physical characteristics in the case of the perovskite structure. To confirm the effect of
15 the structural relaxation on the electronic properties of $Si_{8-n}Sn_n$, we calculated the E-$\boldsymbol{k}$
16 dispersions in the Si_6Sn_2 case without and with the structural relaxation, respectively, as
17 shown in Figs. 4(a) and 4(b). Figure 4(c) shows the Brillouin zone of the unit cell of Si_{8-}
18 $_nSn_n$ and the indication of each axis direction in the $\boldsymbol{k}$-space in this study for reference.
19 Focusing on the degenerated levels of the valence band edge, the triple degenerated
20 levels observed in Fig. 4(a) are broken to double and single levels by considering the
21 structural relaxation, as shown in Fig. 4(b). The degenerated levels on the valence band
22 edge of Si_6Sn_2 are composed of electrons contributed to sp^3 hybrid orbitals

1 corresponding to tetrahedral bonds. This tetrahedral symmetry in the Si_6Sn_2 structure is
2 broken owing to the displacement of Si and Sn atoms with the structural relaxation,
3 which should lead to the breaking of the triple degenerated levels of the tetrahedral
4 structure. We confirmed that these displacements of atoms affect the electronic
5 properties of $Si_{8-n}Sn_n$ for various Sn contents. Even though the displacement of atoms in
6 $Si_{8-n}Sn_n$ is quite small, it affects on the E-$\boldsymbol{k}$ dispersions of $Si_{8-n}Sn_n$. Therefore, the
7 consideration of the structural relaxation is important for correct calculations.
8

9 Up to here, we have discussed the crystalline property of $Si_{8-n}Sn_n$ and the
10 importance of the strain relaxation. Finally, we discussed the E_g of $Si_{8-n}Sn_n$ alloys. In
11 this study, we calculated the E_g values of $Si_{8-n}Sn_n$ alloys with various Sn contents by
12 using the DFT+U method.[26] It is known that E_g is often underestimated by conventional
13 DFT calculation. By introducing on-site Coulomb interaction as a U parameter into
14 electrons on a certain orbit, the electronic state can be corrected empirically. The
15 DFT+U method is usually applied for transition metal oxide compositions, which have
16 d and f electrons[27, 28] because the conventional DFT method can hardly estimate the
17 electronic transition state correctly owing to the discontinuity of the exchange
18 correlation potential.[29–31] Gupta *et al.* have recently calculated the E-$\boldsymbol{k}$ dispersion and
19 carrier mobility of the $Ge_{1-x}Sn_x$ alloy by the DFT+U method. They reported the Sn
20 content dependence of the corrected E_g and x_{dir} of the $Ge_{1-x}Sn_x$ alloy.[32] In this study, to
21 correct the underestimated E-$\boldsymbol{k}$ dispersions of Si and α-Sn, we performed the DFT+U
22 method for electrons on the s-orbit of both Si and Sn, because the underestimated
23 conduction band edge is mainly composed of s-like electronic states. U values were
24 adjusted to be 3.0 and 7.0 eV for Si and Sn, respectively.

1 In view of the effect of the displacement of atoms in $Si_{1-x}Sn_x$ on its electronic
2 properties, to consider the structural relaxation is very important for the E-$\boldsymbol{k}$ calculation.
3 Figure 5 shows the E_g values estimated by the DFT+U method at (a) Γ, (b) X, and (c) L
4 points as a function of the Sn content in $Si_{8-n}Sn_n$. The E-$\boldsymbol{k}$ dispersions of $Si_{8-n}Sn_n$ were
5 calculated for all atomic configurations with the structural relaxation. Then, the
6 calculated E_g results were averaged by considering the formation probability of each
7 point. Note that this result is limited for Sn contents below 65% because the DFT+U
8 calculation does not converge for $Si_{1-x}Sn_x$ with a high Sn content of more than 70%.
9 The direct and indirect bandgaps of $Si_{1-x}Sn_x$ with a Sn content of 25% were theoretically
10 calculated to be 2.1 and 0.5 eV, respectively. However, there is still a discrepancy
11 between those and the experimentally estimated values of 1.05 and 0.83 eV for the
12 direct and indirect E_g, respectively, of polycrystalline $Si_{1-x}Sn_x$ with a Sn content of 18±
13 4%.[8] In this calculation, we use a small unit cell limited to 8 atoms. This model results
14 in a periodic distribution of Sn atoms in unit cells, which may unintentionally affect the
15 E-$\boldsymbol{k}$ structures of $Si_{1-x}Sn_x$ and causes a discrepancy of the energy gap from a practical
16 experimental value. We can see that the E_g values at Γ and L points decrease with
17 increasing Sn content, while the E_g value at the X point seems to increase oppositely.
18 According to these results, the Sn content x_{dir} of the indirect-direct crossover is
19 approximately predicted to be above 50%. There is still variability and a precise x_{dir} is
20 hardly predicted at present (x_{dir}=32–55%).[9–11] Moontragoon *et al.* estimated an x_{dir} of
21 55% by using an empirical pseudopotential method for an 8-atom unit cell.[10] They
22 assumed the virtual crystalline approximation and did not consider the effect of the
23 precise displacement of atomic positions by introducing Sn atoms to Si. Amrane *et al.*
24 predicted an x_{dir} of 49% by using the modified Becke-Johnson exchange correlation

pseudopotential for an 8-atom unit cell[11]. However, they did not consider the atomic displacement of the $Si_{1-x}Sn_x$ alloy. Since we can only calculate the bandgaps of $Si_{1-x}Sn_x$ with an increment step of 12.5% for Sn content, the 8-atom unit cell model is limited to investigate the bandgap of $Si_{1-x}Sn_x$ with minute Sn content. On the other hand, Tolle *et al.* predicted an x_{dir} of 32% by using a 64-atom unit cell model of a $Si_{1-x}Sn_x$ alloy by the scissors correction method.[9] However, they did not report the bandgaps of $Si_{1-x}Sn_x$. To perform a more precise prediction of the energy band structure of a practical $Si_{1-x}Sn_x$ alloy, we believe that the unit cell size should be larger than 64 atoms.

4. Conclusions

We investigated the effect of the average displacement of Si and Sn atoms, $\overline{\Delta r}$, on the lattice constant and E-$\boldsymbol{k}$ dispersion considering all atomic configurations of a $Si_{8-n}Sn_n$ alloy by using the DFT method. We found that a configuration including 1NN Sn atoms is more energetically unstable than that with only 2NN Sn atoms. We calculated the average lattice constant weighted by P_{form} for all atomic configurations of $Si_{8-n}Sn_n$, and the bowing parameter of the lattice constant can be negligibly small compared with those of $Si_{1-x}Ge_x$ and $Ge_{1-x}Sn_x$ binary alloys. We also calculated the E-$\boldsymbol{k}$ dispersion with the structural relaxation and found that the degenerated levels on the valence band edge of Si_6Sn_2 could be broken by breaking the tetrahedral symmetry owing to the displacement of Si and Sn atoms. In addition, from the estimation of E_g corrected by the DFT+U method, the Sn content of the indirect-direct crossover is expected to be above 50%.

Acknowledgements

1 This work was partly supported by a Grant-in-Aid for Scientific Research (S) (Grant No.
2 26220605) from JSPS, the Iketani Science and Technology Foundation, and the Public
3 Foundation of Chubu Science and Technology Center.
4

1 **References**

2 [1]J. Sun, E. Timurdogan, A. Yaacobi, E. S. Hosseini, and M. R. Watts, Nature **493**, 295
3 (2013).
4 [2]C. T. DeRose, R. D. Kekatpure, D. C. Trotter, A. Starbuck, J. R. Wendt, A. Yaacobi, M.
5 R. Watts, U. Chettiar, N. Engheta, and P. S. Davids, Opt. Express **21**, 5198 (2013).
6 [3]G. Sun, H. H. Cheng, J. Menendez, J. B. Khurgin, and R. A. Soref, Appl. Phys. Lett. **90**,
7 251105 (2007).
8 [4]P. Moontragoon, R. A. Soref, and Z. Ikonic, J. Appl. Phys. **112**, 073106 (2012).
9 [5]A. Tonkikh, A. Klavsyuk, N. Zakharov, A. Saletsky, and P. Werner, Nano Res. **8**, 3905
10 (2015).
11 [6]R. A. Soref and C. H. Perry, J. Appl. Phys. **69**, 539 (1991).
12 [7]N. Kobayashi, D. H. Zhu, H. Katsumata, H. Kakemoto, M. Hasegawa, N. Hayashi, H.
13 Shibata, Y. Makita, S. Uekusa, and T. Tsukamoto, Nucl. Instrum. Methods Phys. Res.,
14 Sect. B **121**, 199 (1997).
15 [8]M. Kurosawa, M. Kato, T. Yamaha, N. Taoka, O. Nakatsuka, and S. Zaima, Appl. Phys.
16 Lett. **106**, 171908 (2015).
17 [9]J. Tolle, A. V. G. Chizmeshya, Y. Y. Fang, J. Kouvetakis, V. R. D'Costa, C. W. Hu, J.
18 Menéndez, and I. S. T. Tsong, Appl. Phys. Lett. **89**, 231924 (2006).
19 [10]P. Moontragoon, Z. Ikonic, and P. Harrison, Semicond. Sci. Technol. **22**, 742 (2007).
20 [11]N. Amrane and M. Benkraouda, Am. J. Mater. Sci. Eng. **1**, 12 (2013).
21 [12]R. V. S. Jensen, T. G. Pedersen, and A. N. Larsen, J. Phys.: Condens. Matter **23**,
22 345501 (2011).
23 [13]M. T. Weller, O. J. Weber, P. F. Henry, A. M. D. Pumpoac, and T. C. Hansen, Chem.
24 Commun. **51**, 4180 (2015).

1 [14]K. Cherif, J. Dhahri, E. Dhahri, M. Oumezzine, and H. Vincent, J. Solid State Chem.
2 **163**, 466 (2002).
3 [15]P. G. Radaelli, G. Iannone, M. Marezio, H. Y. Hwang, S-W. Cheong, J. D. Jorgensen,
4 and D. N. Argyriou, Phys. Rev. B **56**, 13 (1997).
5 [16]B. Zhang, C. J. Sun, P. Yang, W. Lu, B. L. Fisher, T. Venkatesan, S. M. Heald, J. S.
6 Chen, and G. M. Chow, Phys. Rev. **89**, 195140 (2014).
7 [17]R. D. Shannon, Acta Crystallogr., Sect. A **23**, 751 (1976).
8 [18]PHASE/0 ver. 3.0 (Institute of Industrial Science, The University of Tokyo, 2015).
9 [19]J. P. Perdew, K. Burke, and M. Ernzerhof, Phys. Rev. Lett. **77**, 3865 (1996).
10 [20]P. E. Bröchl, Phys. Rev. B **50**, 24 (1994).
11 [21]H. J. Monkhorst and J. D. Pack, Phys. Rev. B **13**, 12 (1976).
12 [22]R. Matsuritani, K. Sueoka, and E. Kamiyama, Phys. Status Solidi C **11**, 11 (2014).
13 [23]S. Q. Wangand and H. Q. Ye, J. Phys.: Condens. Matter **15**, L197 (2003).
14 [24]R. Pandey, M. Rérat, and M. Causà, Appl. Phys. Lett. **75**, 4127 (2015).
15 [25]A. Aguado, Phys. Rev. B **67**, 212104 (2003).
16 [26]S. L. Dudarev, G. A. Botton, S. Y. Savrasov, C. J. Humphreys, and A. P. Sutton, Phys.
17 Rev. B **57**, 1505 (1998).
18 [27]E. Finazzi, C. D. Valentin, and G. Pacchioni, J. Chem. Phys. **129**, 154113 (2008).
19 [28]S. Q. Wu, Z. Z. Zhu, Y. Yang, and Z. F. Hou, Comput. Mater. Sci. **44**, 1243 (2009).
20 [29]M. S. Hybertsen and S. G. Louie, Phys. Rev. **34**, 5390 (1986).
21 [30]F. Aryasetiawan and O. Gunnarsson, Rep. Prog. Phys. **61**, 237 (1998).
22 [31]M. Lannoo, M. Schluter, and L. J. Sham, Phys. Rev. B **32**, 3890 (1985).
23 [32]S. Gupta, B. M. Köpe, Y. Nishi, and K. C. Saraswat, J. Appl. Phys. **113**, 073707
24 (2013).

Figure captions

Fig. 1. (color online) Schematic views of a unit cell of a diamond lattice for Si_6Sn_2 alloy consisting of eight atoms with (a) 1NN and (b) 2NN of two Sn atoms.

Fig. 2. (color online) Lattice constant of all atomic configurations of $Si_{8-n}Sn_n$ with the structural relaxation (open diamonds). The average values were weighted by considering P_{form} (green triangles). The lattice constant according to Vegard's law is also indicated by a broken line.

Fig. 3. (color online) Sn content dependence of the $\overline{\Delta r}$ of Si and Sn atoms in $Si_{8-n}Sn_n$ for all configurations (open circles) and the average values weighted by considering P_{form} (orange filled circles).

Fig. 4. (a) Schematic view of the Brillouin zone of a unit cell consisting of 8 atoms. E-$\boldsymbol{k}$ dispersions of Si_6Sn_2 (b) without and (c) with the structural relaxation.

Fig. 5. Sn content dependence of the energy bandgaps at the (a) Γ, (b) X, and (c) L $\boldsymbol{k}$-points of $Si_{8-n}Sn_n$. Open symbols show E_{g} for all atomic configurations. The closed symbol shows the average E_g value weighted by considering P_{form}.

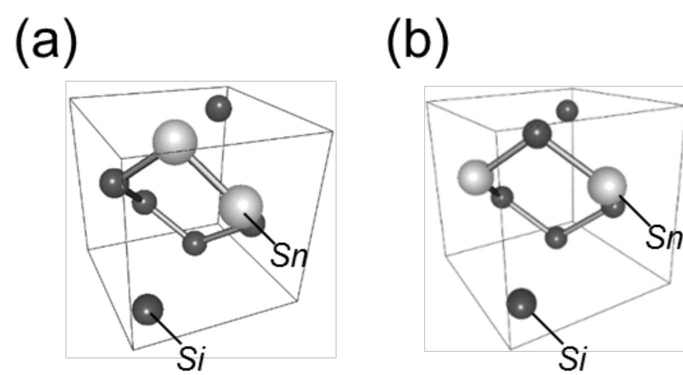

1
2
3
4
5 Fig. 1
6
7

1

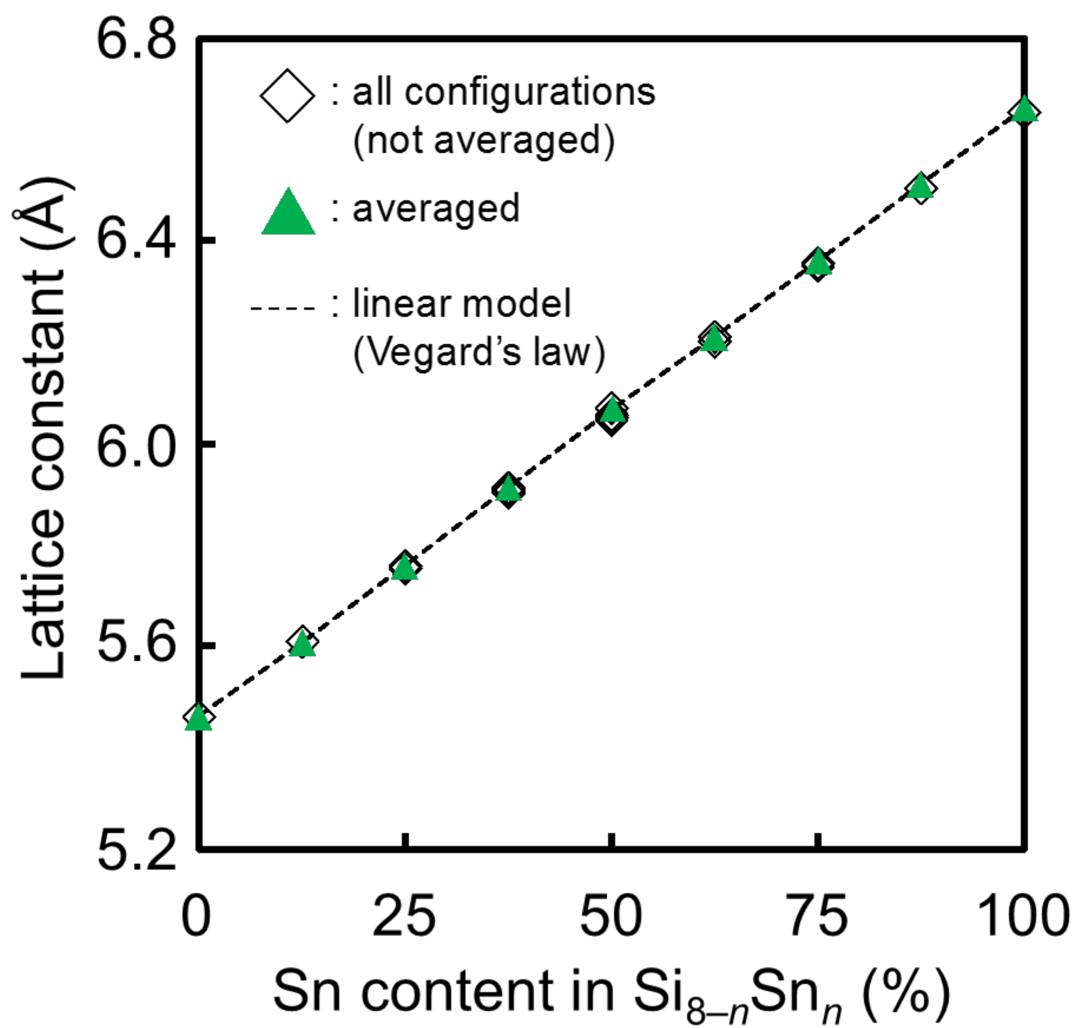

2

3 Fig. 2

4

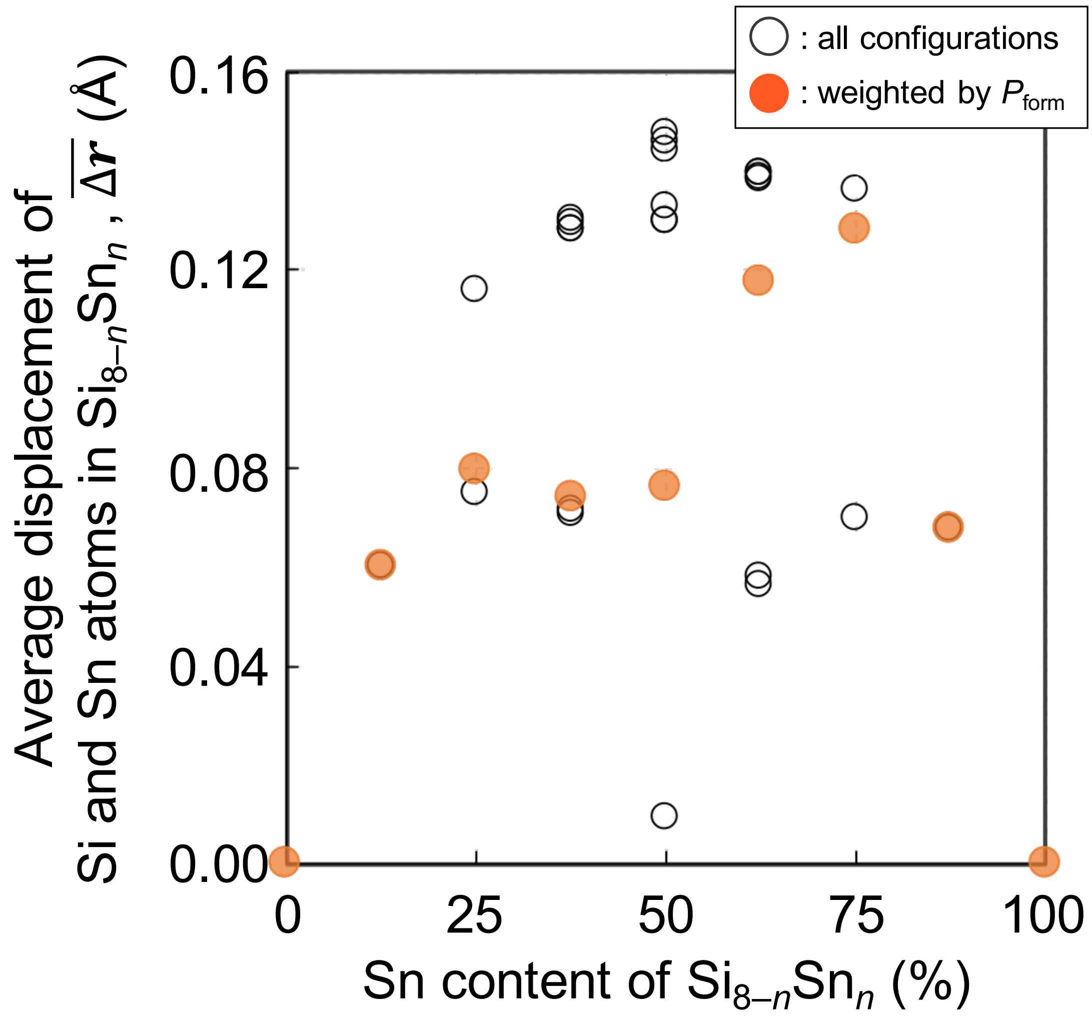

1

2

3

4 Fig. 3

5

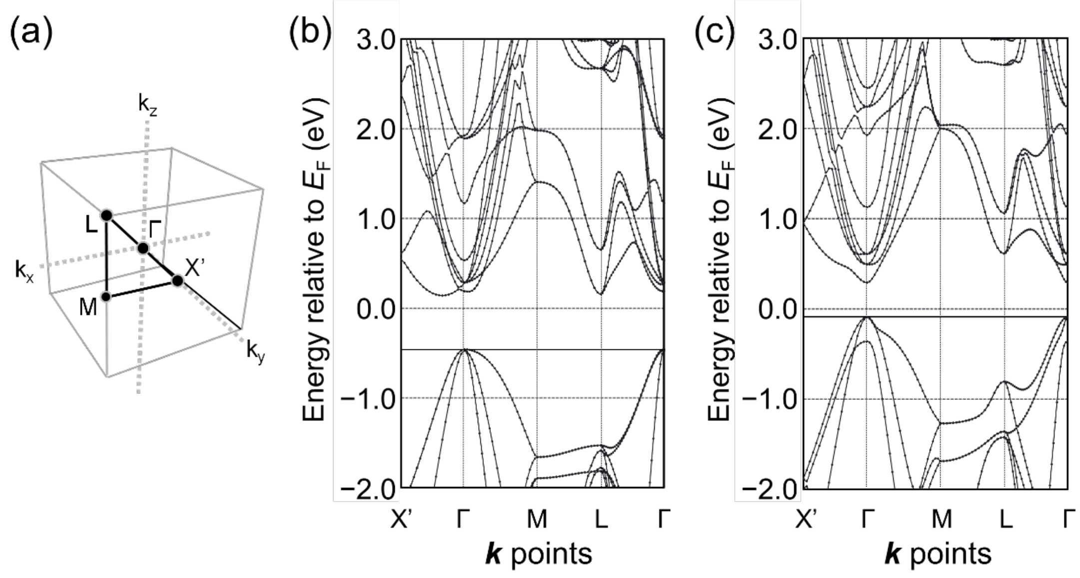

1

2

3

4 Fig. 4

5

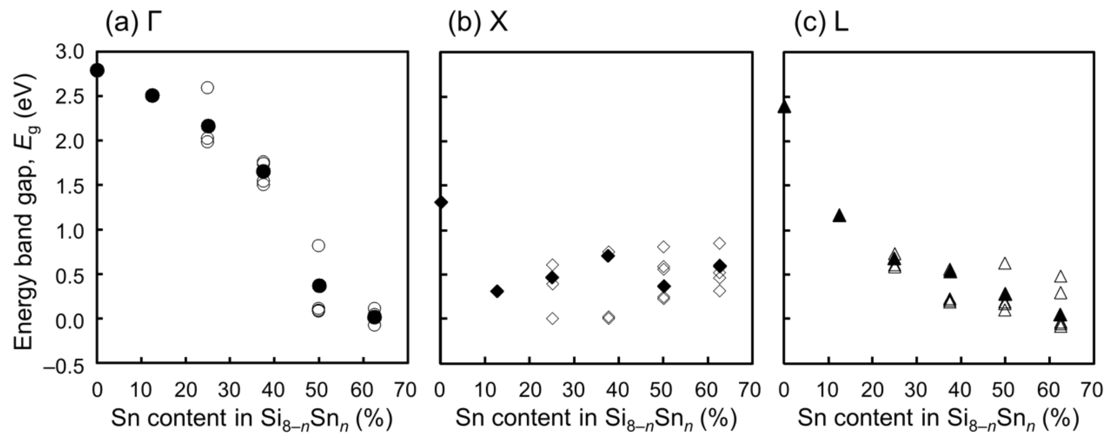

1
2
3
4
5 Fig. 5
6